Continuum theory of the mixed-state and surface Joule effects in type-II superconductors

T. Hocquet, P. Mathieu, and Y. Simon
Laboratoire de Physique de la Matière Condensée de l'Ecole Normale Supérieure, F-75231 Paris CEDEX 05, France
(Received 30 October 1991)

A phenomenological theory of vortex motion, where the mixed state is regarded as a continuum, has been proposed by two of the authors in a short previous letter. Its outlines are recalled in this paper with further comments and arguments; in particular the basic equations and their implications are discussed at some length. This theory leads to a model of pinning, from which we argue that critical currents I_c, in soft type-II samples of standard bulk homogeneity, should be governed essentially by surface defects. I_c is interpreted as a physically well-defined part of the total transport current I, which is flowing over a small depth close to the surface. Thus, on the scale of an ordinary sample, this part of the transport current is superficial, the remaining part $I-I_c$ being uniformly distributed over the cross section. Coherently, an analysis of the dissipation in such samples predicts that the part VI_c of the total Joule effect VI must arise as surface heat sources, while the Joule effect $V(I-I_c)$, usually associated with the steady viscous flow of vortices, is uniformly distributed in the bulk. As a proof, we present a method, using second-sound acoustics, to detect and separate surface and volume heat sources. Experimental results give clear evidence of a surface Joule effect, and support the validity of our model of surface pinning in soft materials.

I. INTRODUCTION

It is difficult to separate the effects in vortex pinning of surface and volume defects, which are generally presumed to coexist in any sample. However, a number of experiments in the past clearly demonstrated the importance,[1] if not the exclusive role,[2] of surface defects in determining the relatively small critical currents of soft type-II superconductors.

In soft samples, the notion of critical current density J_c, when given crudely as the ratio I_c/S of critical current over cross-sectional area, clearly is inadequate. It presupposes the macroscopic transport current density to be uniform; at best J_c gives a rough indication of critical properties. In this respect the results obtained by Joiner and Kuhl[2] are quite instructive. The authors reported that J_c's of a series of PbBi foils were linear in the surface-to-volume ratio, or equivalently in the perimeter–to–cross-section ratio, $2w/S$. From this, they were led to the conclusion that, in their words, the surface was the major determinant in the flux pinning. By expressing their data in terms of J_c, Joiner and Kuhl somewhat obscured the striking and simple result, that foils with various thicknesses, otherwise prepared in the same way, had a constant critical current. Their conclusion was furthermore too weak. In view of their results, they could have claimed that the surface of the foils was the sole source of pinning. According to a naive critical-state model, an applied current from 0 to I_c, should flow on the surface. If that is the case, the more relevant parameter would be a superficial critical current density, $i_c=I_c/2w$ (in A/m),[3] measuring the ability of the surface to transport a supercurrent over a small depth without dissipation.

In the concluding remarks of Sec. V, we shall argue that such samples, in which surface defects practically determine critical currents, and which we shall refer to as "*soft*" in this paper, are not exceptional, nor do they correspond to some limiting, and seldom attained, metallurgical state. We think that, in fact, a wide class of materials including most of those used in fundamental measurements (transport properties, thermomagnetic effects, flux-flow noise, etc.), which are soft in the common sense, i.e., have low to moderate I_c, can also be regarded as *soft* in the above restricted sense.

Thus, in characterizing soft samples, the first thing is to know where the applied current flows. Two methods have been proposed to investigate the spatial current distribution on the scale of the sample. The first one,[4] which we have repeated as a preliminary test for our PbIn rods, consists in measuring the small magnetic field due to the transport current itself; miniature pickup coils placed on the surface of a specimen of large cross section were used. When I is increased from zero, it was observed that the current distribution evolves from a zero-field London distribution (superficial) for low currents, to a volume normal distribution for large currents ($I \gg I_c$). The second method[5] used neutron diffraction from the flux-line lattice. The neutron beam was directed along the external field and the broadening of the rocking curves (angular intensity distribution when rotating the sample) reflected the bending of flux lines associated with the transport current density $\mathbf{J}$, according to Ampere's law $\mathrm{curl}\mathbf{B}=\mu_0\mathbf{J}$. From the three NbTa slabs measured in Ref. 5, the one denoted as sample 1 was distinctly soft, while the other two were not. In some respects, both methods may have appeared not to be entirely conclusive. Various current distributions might have given the same signal in a pickup coil, or the same width of the rocking curve. The first method, contrary to the second, is straightforward to interpret, and unambiguous in the limits $I \to 0$ and $I \to \infty$;

however, in the flux-flow regime, one is unable to determine how much, if any, of the transport current still is flowing on the surface.

In Sec. IV, we present a third method to demonstrate that, in normally homogeneous samples, a constant part $I_1 \simeq I_c$ of the applied current, in the flux-flow regime, is flowing on the surface, while the remaining part, $I_2 \simeq I - I_c$, is uniformly distributed in the bulk. In this case, it is to be expected that the Joule power VI, where $V = R_f I_2$ is the flux-flow voltage, should have the same spatial distribution that the transport current itself. The second-sound experiment described in Sec. IV was designed to measure and locate the Joule heat sources. A sample of large cross section is immersed in a superfluid helium bath, at 1.7 K, and an ac current is superimposed to the main dc current. The low frequency used (from 0.5 to 1 kHz) ensures a quasistatic modulation of the V-I characteristic, as also of the related heat sources. Thus, second-sound waves are emitted from the sample through He II, and can be accurately investigated after amplification by a resonant cavity. In the working frequency range, in contrast with electrical properties, thermal inertial effects become important, the thermal skin depth being relatively small on the scale of the sample. As a result, second-sound signals have different and well-defined phases, depending on whether their sources are uniformly distributed throughout the sample or superficial, and thereby can be easily separated experimentally. In spite of this roundabout way of measuring heat sources, as it may appear to someone unfamiliar with second-sound acoustics, experimental evidence of a surface Joule effect can be regarded as the most direct and unambiguous demonstration of the *soft behavior* such as defined above.

Recently two of us (P.M. and Y.S.) have developed a theory of vortex motion,[6] where the mixed state is treated as a continuum. When applied to soft samples, jointly with a surface pinning model, the Mathieu-Simon (MS) theory accounts for the order of magnitude of critical currents,[6] as well as for their field and temperature dependence.[3] As discussed in Sec. III, it also explains experimental results on the distribution of currents and Joule dissipation, such as we have observed. Through the example of soft samples, we also hope to bring out the relevance of the MS phenomenological theory in tackling pinning and transport problems in type-II superconductors.

Using a rigorous standard method, based upon conservation laws, MS derived conditions of equilibrium and a complete system of transport equations in the mixed state. This approach is very similar to that used by Bekarevitch and Khalatnikov[7] (BK) to describe vortex motion in He II. As far as we know, no real attempts in this direction have been made before. In a paper concerned with collective oscillations of vortices in superconductors, Abrikosov *et al.*[8] did transcribe the BK equation of superfluid motion including the analog of the mutual-friction force; but arguing from analogy they obtained approximate and, moreover, restricted results. Superconductors and superfluid helium have many features in common, and it is clear that a parallel between the two systems can be very instructive. Indeed, the MS model also took ample advantage of such a comparison. We emphasize, however, that the point here was more to apply to both cases, rotating He II and the mixed state, the same general and rigorous procedure, best suited to both systems, than merely relying on rather limited analogies, especially when dealing with electromagnetic properties of the mixed state.

Otherwise, several other continuum descriptions of type-II superconductors have been worked out, either in equilibrium[9] or with dissipative processes taken into account.[1,10] In spite of formal similarities in writing equations of transport and dissipation, these exhibit fundamental differences with the MS theory, in particular, in the physical interpretation of magnetization and the distinction between diamagnetic and transport currents. These differences may have escaped the reader in a short letter,[6] and require further comments. Therefore, the physical meaning of the MS equations will be discussed at some length in Sec. II.

Moreover, the MS theory was presented in Ref. 6 in the simplified frame of the so-called "London model," assuming extreme type-II materials ($\kappa \gg 1$ or $\lambda \gg \xi$) in the intermediate range of fields ($H_{c1} \ll H_0 \ll H_{c2}$). This restriction, in fact, was unnecessary and, as shown in Sec. II, this theory applies to more general situations.

II. PHENOMENOLOGICAL THEORY OF THE MIXED STATE

A. The macroscopic London equation

Recall that one original aim of the BK theory[7] was to derive phenomenologically, according to an idea advanced by Landau, the elastic forces on vortices in He II. These forces were introduced by Hall in analyzing transverse wave motion of vortices in an oscillating disks experiment. Also, in type-II superconductors, a continuum theory is most suitable to handle situations where the vortex lattice is distorted, as it is necessarily the case in the vicinity of defects, or even, as we shall see, in an ideal sample near its surface.

In such circumstances, the first important thing to realize is that, in general, vortex lines (VL), even at equilibrium, do not necessarily coincide with flux lines. This becomes evident in writing the macroscopic London equation, such as derived below in Eq. (3).

When a type-II sample is immersed in an external magnetic field $\mathbf{H}_0$ ($=\mathbf{B}_0/\mu_0$), generally intricate and intractable distributions of the order parameter $\psi = \rho e^{i\theta}$, of microscopic supercurrents $\mathbf{j}_S$ and electromagnetic fields $\mathbf{e}, \mathbf{b}$, arise throughout the body. *Microscopic* or *macroscopic* here meaning on a small or large scale compared with the vortex spacing a. In describing the local state of the vortex lattice, regarded as a continuum, by a reduced number of macroscopic variables, one avoids dealing with details of the microscopic vortex structure. Cross-grained mean values of $\mathbf{j}_S$, $\mathbf{e}$, and $\mathbf{b}$, will be denoted as capital letters $\mathbf{J}_S = \langle \mathbf{j}_S \rangle$, $\mathbf{E} = \langle \mathbf{e} \rangle$, and $\mathbf{B} = \langle \mathbf{b} \rangle$. It will be also convenient to introduce the superfluid velocity $\mathbf{v}_S$ defined by

$$\mathbf{j}_S = n_S q \mathbf{v}_S = n_{S0} q f^2 \mathbf{v}_S$$

as well as its local spatial average, $\mathbf{V}_S = \langle \mathbf{v}_S \rangle$. Here $q = -2e$ is the effective charge, $n_S = \rho^2$ is the superfluid density, n_{S0} the zero-field equilibrium value of n_S, and f is the reduced order parameter.

The current equation of the Ginzburg-Landau (GL) theory relates $\mathbf{j}_S$, or $\mathbf{v}_S$, to the phase of the order parameter:

$$\begin{aligned} &2m\mathbf{v}_S = \hbar\nabla\theta - q\mathbf{a} , \\ &\mathbf{a} - \frac{m\mathbf{v}_S}{e} = \frac{\hbar\nabla\theta}{q} = -\frac{\varphi_0}{2\pi}\nabla\theta , \end{aligned} \tag{1}$$

where $\mathbf{a}$ is the vector potential, m the electron mass, and φ_0 the flux quantum. Taking the curl of Eq. (1), one obtains

$$\mathbf{b} - \frac{m}{e}\mathrm{curl}\mathbf{v}_S = 0 \tag{2}$$

everywhere, except at the vortex cores. Equation (2), which we may refer to as the first London equation, states that the momentum field of the supercurrent, $\mathbf{p}_S = \hbar\nabla\theta$, is irrotational. Like its superfluid analog, $\mathrm{curl}\mathbf{v}_S = 0$, it appears as a constitutive relation characteristic of the superconducting state, whether at equilibrium or not. We stress that Eq. (2) is valid in the whole range of fields, wherever $f \neq 0$ and do not imply the approximations of the London model ($f = 1$, outside the cores; extreme type-II materials).

Consider a vortex continuum and let n be the local vortex density (defined as the VL length by volume unit), and $\boldsymbol{\nu}$ the unit vector along the VL. The macroscopic average of Eq. (2), taking account of singularities, reads

$$\mathbf{B} - \frac{m}{e}\mathrm{curl}\mathbf{V}_S = \boldsymbol{\omega} = n\varphi_0\boldsymbol{\nu} . \tag{3}$$

Similarly, in rotating He II,[7] $\mathrm{curl}\mathbf{V}_S = \boldsymbol{\omega}$, on substituting the quantum of circulation h/m to φ_0 in $\boldsymbol{\omega}$. To show that Eq. (3) does indeed represent the correct average of the microscopic London equation, consider a familiar magnetostatic analog: an array of infinitesimal filaments (density n, direction $\boldsymbol{\nu}$), each of them carrying a current $i_0^* = \varphi_0$, so that the resulting macroscopic current density is $\mathbf{J}^* = n i_0^* \boldsymbol{\nu} = \boldsymbol{\omega}$. Here the microscopic field $\mathbf{b}^*/\mu_0$ is the analog of $\mathbf{p}_S/q$; its circulation around a filament is $i_0^* = \varphi_0$, whereas $\mathrm{curl}\mathbf{b}^*/\mu_0 = 0$ outside. Now, one usually takes for granted that the macroscopic field $\mathbf{B}^*$ obeys macroscopic Amperes's law, $\mathrm{curl}\mathbf{B}^*/\mu_0 = \mathbf{J}^*$, which is the counterpart of Eq. (3).

B. The thermodynamic identity and the vortex potential ε

According to MS,[6] the macroscopic density of free energy, in the mixed state, $\bar{F}$, can be expressed as function of a few macroscopic parameters, such as those defined above, $\mathbf{E}$, $\mathbf{B}$, $\mathbf{V}_S$ (or $\mathbf{J}_S$), $\boldsymbol{\omega}$, and the temperature T and the total electronic density $N_e = \bar{n}_e$ ($-n_e e$ is the microscopic space charge):

$$\bar{F} = \bar{F}(T, N_e, \mathbf{E}, \mathbf{B}, \mathbf{V}_S, \boldsymbol{\omega}) . \tag{4}$$

In comparison with He II, the task is partly simplified, since, due to the lattice, a *single* flow, the supercurrent $\mathbf{J}_S$ (or $\mathbf{V}_S$), will appear in the set of independent thermodynamic variables, instead of two, $\mathbf{V}_S$ and $\mathbf{V}_n$, in helium. In irreversible processes, a normal current $\mathbf{J}_n = \mathbf{J} - \mathbf{J}_S$ can possibly occur, but $\mathbf{J}_n$ will be regarded as a flux. On the other hand, complications arise because of the electromagnetic terms.

Expression (4) needs some comment. Equation (3) and Maxwell-Ampere's law are primary constraints, limiting the possible spatial variations of currents and fields throughout a vortex lattice, whether at equilibrium or not. Nevertheless, $\mathbf{B}$, $\mathbf{J}_S$ (or $\mathbf{V}_S$), and $\boldsymbol{\omega}$, must be considered, locally, as independent variables: for fixed values of $\boldsymbol{\omega}$ and $\mathbf{V}_S$ at some point M, $\mathbf{B}(M)$ still may be varied by any change in the distribution of currents elsewhere. It might turn out that equilibrium conditions for the body as a whole require that $\boldsymbol{\omega} = \mathbf{B}$ [and/or $\mathrm{curl}\mathbf{V}_S = 0$, in accordance with Eq. (13)]. But, to decide this, we first have to minimize (with constraints) the relevant thermodynamic potential by precisely using some general expression of $\bar{F}$ in the form (4).

In Eq. (4), intended to describe equilibrium states as well as flux flow, the order parameter has been removed from the set of independent macroscopic variables. This implies that $f(\mathbf{r}, t)$ rigidly satisfies its equilibrium conditions, as if it relaxed instantaneously. Strictly f obeys some time-dependent GL equation, for instance, of the simple type considered by Schmid:[11]

$$\frac{\partial f}{\partial t} = -\frac{L}{2\tau} = -\frac{1}{2\tau}\left[f - f^3 - \frac{f\xi^2}{\hbar^2}(\hbar\nabla\theta - q\mathbf{a})^2 + \xi^2\Delta f \right] , \tag{5}$$

where L is the left-hand side of the first GL equation, acting as a generalized force in the sense of irreversible thermodynamics, and τ is the relaxation time of the superfluid density $n_S = \rho^2$. At temperatures not too close to T_c, τ does not exceed 10^{-12} sec.[11] In practical conditions, $L \sim \tau\dot{f} \sim \tau(v_L/a)f$, where $v_L = E/B$ is the VL velocity, so that $L/f \sim \tau v_L/a \sim 10^{-5}$–$10^{-6}$ is negligible ($L \ll f$). Or equivalently stated, $L \simeq 0$, within an accuracy 10^{-5}–10^{-6}; in this sense, f hardly departs from equilibrium. In contrast, but consistently, the contribution of time-relaxation effects to dissipation[11] remains significant ($\mu_0 H_c^2 L^2/\tau$ in W/cm^3).

By using only the parameter $\boldsymbol{\omega}$ to describe the vortex lattice, just as BK do in He II, we ignore small differences in energy between, for example, triangular and square lattices. This approximation relies on the smallness of the calculated elastic constant C_{66},[1] associated to shear in a plane perpendicular to VL. We emphasize, however, that other elastic effects, due to compression and torsion of the vortex lattice, are involved in Eq. (4).

A local value of the macroscopic free-energy density $\bar{F}(M)$, or of its differential $d\bar{F}$, can be obtained by averaging the GL expression for the microscopic free-energy density F (or dF) over an element of volume τ around the point M, which is small on the macroscopic scale, but enclosing many vortices:

$$d\bar{F}=\frac{1}{\tau}\int_{\tau} dF_{\mathrm{GL}} \ . \tag{6}$$

If there is no ambiguity, the differential symbol d^3r under the integral sign will be omitted.

Consider an infinitesimal process leaving the VL array unaltered in the neighborhood of M; even assuming that the lines $f=0$ remain fixed, the microscopic fields $f,\mathbf{b},\mathbf{v}_S,\ldots$ still may undergo infinitesimal changes, resulting in infinitesimal changes in all macroscopic variables $\mathbf{B},\mathbf{V}_S,\ldots$, except ω which is constant. To calculate $d\bar{F}$ in such a process we may take τ as a bundle of vortex cells of unit length, and use periodic boundary conditions. Thus, allowing for Eq. (1) and the first GL equation, $L=0$, integral (6) reduces to

$$d\bar{F}=\frac{1}{\tau}\int_{\tau} -\sigma\, dT+\mu dn_e+\epsilon_0\mathbf{e}\cdot d\mathbf{e} +\frac{1}{\mu_0}\mathbf{b}\cdot d\mathbf{b}-\frac{m}{e}\mathbf{j}_S\cdot d\mathbf{v}_S \ , \tag{7}$$

where μ is the chemical potential of the electrons, and σ the entropy density. Note that, because of the expected smallness of the electrostatic or space-charge effects, the second and third terms in the integrand of (7) are usually omitted in writing the GL free energy. Yet, we have preferred to restore them here for a general and clear derivation of equilibrium conditions.

Excluding microscopic temperature gradients, further manipulation of (7), and use of Maxwell equations leads to[12]

$$d\bar{F}=-\bar{\sigma}dT+\bar{\mu}dN_e+\epsilon_0\mathbf{E}\cdot d\mathbf{E}+\frac{1}{\mu_0}\mathbf{B}\cdot d\mathbf{B}-\frac{m}{e}\mathbf{J}_S\cdot\mathbf{V}_S \ .$$

This is the differential of $\bar{F}$ at constant ω. It may be noted that the macroscopic electromagnetic energy separates and $\mathbf{J}_S$ appears as the conjugate variable of $\mathbf{V}_S$. In any process involving vortex motion and change in VL density, we shall write

$$d\bar{F}=-\bar{\sigma}dT+\bar{\mu}dN_e+\epsilon_0\mathbf{E}\cdot d\mathbf{E}+\frac{1}{\mu_0}\mathbf{B}\cdot d\mathbf{B} -\frac{m}{e}\mathbf{J}_S\cdot d\mathbf{V}_S+\boldsymbol{\varepsilon}\cdot d\boldsymbol{\omega} \ , \tag{8}$$

where $\boldsymbol{\varepsilon}=\partial\bar{F}/\partial\boldsymbol{\omega}$ will be referred to in this paper as the VL *potential*. It is clear that any description of the vortex state, where $\boldsymbol{\omega}$ and $\mathbf{B}$ are not differentiated, would lead one to adopt another definition of the VL chemical potential.[1] Similarly $d\bar{U}=Td\bar{\sigma}+\cdots$, where $\bar{U}$ is the energy density.

Assuming $N_e\simeq 0$, $\boldsymbol{\varepsilon}$, in general, will be a function of T, $\boldsymbol{\omega}$, and $\mathbf{V}_S$. In many practical situations, however, the $\mathbf{V}_S$ dependence of $\boldsymbol{\varepsilon}$ may be ignored or neglected as a first estimate, so that the VL potential of a perfect uniform lattice, for which $\mathbf{V}_S\equiv 0$ ($\mathbf{J}_S\equiv 0$), provides a good approximation for $\boldsymbol{\varepsilon}$. Such is the case, as we shall see, in the bulk of the sample, and, in general wherever low current densities and small deformations of the VL lattice are involved.[3,12] On the other hand, if the London model applies, ($\xi\ll a\ll\lambda$), $\mathbf{J}_S=n_{S0}q\mathbf{V}_S$ is $\boldsymbol{\omega}$ independent, and $\partial\boldsymbol{\varepsilon}/\partial\mathbf{V}_S=0$ accordingly, for any value of $\mathbf{V}_S$. In an isotropic material, $\boldsymbol{\varepsilon}=\boldsymbol{\varepsilon}(\omega,T)$ necessarily has the same direction as $\boldsymbol{\omega}$, and then the last term in Eq. (8) can be rewritten as

$$\boldsymbol{\varepsilon}\cdot d\boldsymbol{\omega}=\varepsilon\boldsymbol{\nu}\cdot d\boldsymbol{\omega}=\varepsilon d\omega=\varepsilon\varphi_0 dn \tag{9}$$

to be compared with the term $\lambda d\omega$ in the BK thermodynamic identity of rotating He II.[7]

In a uniform lattice, the classical relation $\boldsymbol{\omega}=\mathbf{B}$ ($B=n\varphi_0$) holds, in agreement with Eq. (3), since $\mathbf{V}_S\equiv 0$. Expression of its free-energy density, $\bar{F}(B)$, expressed (at a given T) as function of the single parameter $\boldsymbol{\omega}=\mathbf{B}$, have been calculated in some limiting cases.[13] The corresponding VL potential $\varepsilon(\omega)$ follows immediately on identifying $\mathbf{B}/\mu_0+\boldsymbol{\varepsilon}$ with $\partial\bar{F}/\partial\mathbf{B}$. The formation free energy per unit length of an isolated VL is $\varphi_0 H_{c1}$; hence, the limiting value $\varepsilon\to H_{c1}$ as $B\to 0$ (Fig. 1). In the intermediate range of fields ($H_{c1}\ll H_0\ll H_{c2}$), according to the London model

$$\varepsilon=\frac{\varphi_0}{4\pi\mu_0\lambda^2}\ln\left[\frac{a}{\xi^*}\right] \ , \tag{10}$$

where $a^2\sim\varphi_0/\omega$ and $\xi^*\gtrsim\xi$ is an effective core radius. For Abrikosov's triangular lattice, near H_{c2},

$$\varepsilon=\frac{H_{c2}-\omega/\mu_0}{1.16(2\kappa_2^2-1)+1} \ , \tag{11}$$

where κ_2 is the second generalized GL parameter.

In rationalized units, ω and $\mathbf{B}$ are both expressed in T, so that $\boldsymbol{\varepsilon}$ is expressed in A/m, just as a field $\mathbf{H}$ or a magnetic density $\mathbf{M}$. Some authors (while taking $\boldsymbol{\omega}\equiv\mathbf{B}$) introduced a thermodynamic $\mathbf{H}$ field at any point as $\nabla_{\mathbf{B}}\bar{F}$. The related idea here would be to define a magnetization $\mathbf{M}$ as $\nabla_{\boldsymbol{\omega}}\bar{F}$, i.e., $\mathbf{M}=-\boldsymbol{\varepsilon}$. As a matter of fact, the curve ε vs ω/μ_0 for a regular lattice, such as shown in Fig. 1, is

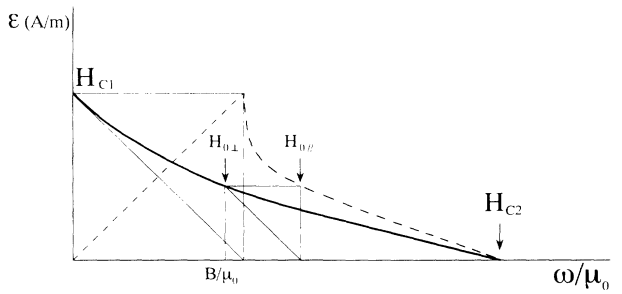

FIG. 1. The local vortex potential ε vs ω/μ_0 for a uniform vortex lattice ($\omega=n\varphi_0=B$) such as defined by Eqs. (8) and (9); $\varepsilon(B,T)$ is the fundamental equation of state that involves the magnetic properties of a type-II sample. The curve ε vs ω/μ_0 coincides with the magnetization curve $-M$ vs H_0 of a slab perpendicular to the external field $\mathbf{H}_0$ ($B=B_0=\mu_0 H_0$). As for the classical reversible magnetization curve (dashed line), it concerns the equilibrium of a perfect cylinder parallel to $\mathbf{H}_0$. Both curves are deduced from each other by a simple construction as shown, according to the implicit equation $-M=\varepsilon(H_0+M)$.

simply related to the usual reversible magnetization curve [note that $\varepsilon(\omega/\mu_0)=-M(H_0)$ is positive]. Nevertheless, we shall take care not to confuse the concept of vortex potential, which has a precise and unambiguous thermodynamic definition, with some macroscopic magnetization $\mathbf{M}$, which actually has no local sense in a superconductor. The relationship $\varepsilon=\varepsilon(\omega,T)$ should be regarded as the fundamental equation of state, whereas the equality $M(H_0)=-\varepsilon(\omega/\mu_0)$ represents a condition of thermodynamic equilibrium for a simple shaped sample taken as a whole. In our opinion, the introduction of $\mathbf{M}$ and $\mathbf{H}$ as local quantities in the mixed state not only is unnecessary but also contains a number of pitfalls; we shall return to this point below.

C. Equilibrium of a perfect sample

As pointed out in Ref. 1, there has been some confusion in the literature concerning the choice of the reliable thermodynamics potential used to determine the equilibrium of a type-II sample. So the question is worth being restated here, even briefly.

Consider (at constant T) an insulated body, immersed in an external field $\mathbf{H}_0$. Suppose that $\mathbf{H}_0$ is produced by currents $\mathbf{J}_0$ in a zero-resistance coil, which is driven by an ideal generator; i.e., a source of emf, adjustable at will, and acting as a reversible work source (no entropy). During *any* process affecting the body, the work done by the generator to overcome the induced electric field is

$$\delta W=\int_{\text{coil}}-\mathbf{E}\cdot\mathbf{J}_0\delta t=\int_{\text{all space}}\mathbf{H}_0\cdot\delta\mathbf{B}\ . \tag{12}$$

The second equation in (12) is a straightforward consequence of Maxwell equations. When $\mathbf{H}_0$ is kept constant, $\mathbf{H}_0\cdot\delta\mathbf{B}=\delta(\mathbf{H}_0\cdot\mathbf{B})$, and $-\mathbf{H}_0\cdot\mathbf{B}$, integrated over all space, can be taken as measuring the energy level of the generator. Let $\mathcal{F}$ be the total free energy of the body and space, obtained by integrating some free-energy density $\bar{F}$ over the body and $\mathbf{B}^2/2\mu_0$ outside. At constant $\mathbf{H}_0$, the magnetic free enthalpy defined as

$$\mathcal{G}=\mathcal{F}-\int_{\text{all space}}\mathbf{H}_0\cdot\mathbf{B} \tag{13}$$

represents nothing but the free energy of the total system consisting of the body and space plus the electrical generator (excepting the heat reservoir), which must be minimum at equilibrium. We stress that this equilibrium criterion holds for *any* sample, taken as a whole, whatever its shape or kind may be. Now for a (para, ferro) magnetic material, where a magnetization $\mathbf{M}$ is clearly defined, it is useful to introduce a local $\mathbf{H}$ field, $\mathbf{H}=\mathbf{B}/\mu_0-\mathbf{M}$. Then, as easily shown, $\mathbf{H}$ may be substituted for $\mathbf{H}_0$ in Eqs. (12) and (13); this alternative expression for $\mathcal{G}$ is generally preferred in such materials because of a local relationship between $\mathbf{M}$ (or $\mathbf{H}$) and $\mathbf{B}$, which is unfounded in a superconductor.

Minimizing $\mathcal{G}$ against small variations of N_e, $\mathbf{E}$, $\mathbf{B}$, $\mathbf{J}_S$, and ω, subject to proper constraints (charge conservation, London and Maxwell equations), the following equilibrium conditions are derived:

$$\mathbf{E}'=\mathbf{E}+\frac{\nabla\mu}{e}=0\ , \tag{14}$$

$$\varepsilon\times\mathbf{N}=0\ , \tag{15}$$

$$\mathbf{C}=\mathbf{J}_S+\text{curl}\varepsilon=0\ . \tag{16}$$

Equation (14) states, as usual, that $\mathbf{E}'$, the gradient of the electrochemical potential, is zero. Equations (15) and (16) express, in macroscopic form, the equilibrium of VL. In the boundary condition (15), $\mathbf{N}$ is the normal unit vector. To interpret them more easily, let us assume that the *London model* applies ($\varepsilon=\varepsilon\boldsymbol{\nu}$), so that Eqs. (15) and (16) become

$$\boldsymbol{\nu}\times\mathbf{N}=0\ , \tag{17}$$

$$\mathbf{J}_S+\text{curl}\varepsilon\boldsymbol{\nu}=0\ . \tag{18}$$

Plaçais and two of us[14] derived two similar equations in rotating He II that involve the same physical interpretation [see Eqs. (11) and (12) in Ref. 14]. The boundary condition (17) states that vortices terminate perpendicular to the sample surface as shown in Fig. 2 (or to cavity walls in He II). This holds on a microscope scale and can be understood by considering the interaction between a VL and its image.[6] In Eq. (18), the quantity $\mathbf{C}$ may be regarded as a macroscopic expression for the local supercurrent $\mathbf{j}_{S0}$ "applied" at the core of a VL, including that induced by the vortex itself if it is curved. It is well known from microscopic theory of flux flow,[15] that a VL indeed moves as soon as $\mathbf{j}_{S0}\neq 0$. For instance, in the limiting case of low fields and quasi-isolated VL ($\varepsilon\to H_{c1}$), a homogeneous bending of the VL lattice would induce at the vortex cores a current $\mathbf{j}_{S0}=H_{c1}\boldsymbol{\nu}\times\mathbf{u}/R$ (where $\mathbf{u}$ is the principal normal and R the radius of curvature); this expression taken from Ref. 15 can be rewritten as $\mathbf{j}_{S0}=H_{c1}\text{curl}\boldsymbol{\nu}=\text{curl}\varepsilon\boldsymbol{\nu}$.

Figure 2 sketches the *one* equilibrium structure of the VL lattice such as expected from the above set of equations.[6] In a simple shaped sample (sphere, cylinder,...), VL in the bulk will be uniformly distributed with constant values $\boldsymbol{\nu}=\boldsymbol{\nu}_1$, $\varepsilon=\varepsilon_1$, giving $\mathbf{J}_S\equiv 0$ and $\boldsymbol{\omega}_1\equiv\mathbf{B}_1$. But, in order to satisfy the boundary condition (17), VL bend to end normal to the surface. The deformation of the VL lattice takes place over a small depth d from the surface.

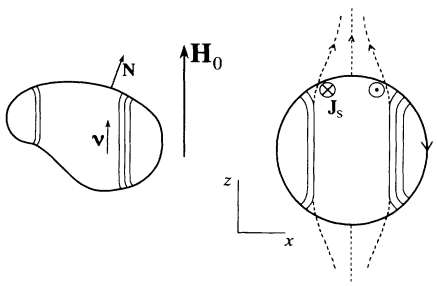

FIG. 2. Schematic of the equilibrium vortex distribution in a perfect sample. Vortex lines curve in over a small depth near the surface to end normal to the boundary [see Eq. (17)]; correlatively spontaneous diagmagnetic currents J_S ensure vortex equilibrium as required by Eq. (18). In this perturbed layer the lines of force of the magnetic field (dashed lines) strongly deviate from vortex lines, in agreement with the macroscopic London equation (3).

In the London model, from Eqs. (3), (10), (17), and (18), with $\mathbf{J}_S = n_{S0} q \mathbf{V}_S$, d is found to be of the order of $\lambda(\varepsilon\mu_0/\omega)^{1/2} \sim a(\ln a/\xi^*)^{1/2}$.[6] In accordance with Eq. (18), Meissner-like (diamagnetic) currents $\mathbf{J}_S$ flow near the surface. It is to be emphasized that, inside the perturbed layer d, where $\omega \neq \mathbf{B}$, VL are not flux lines; both fields lines and VL incurve, but in opposite directions (Fig. 2).

Superfluid vortices in rotating He II behave similarly. The bending of vortices near the plane walls of a cavity, inclined to the axis of rotation, results in a spectacular decrease of the vortex density along the walls (see Fig. 1 of Ref. 14). This expectation was confirmed by accurate second-sound measurements.[14] Also in He II, the characteristic depth d is not much larger than the vortex spacing a. Therefore, one might question the relevance of a continuum theory to describe such effects. However, the observed quantitative agreement between second-sound data and predictions of the continuum model in He II (Ref. 14) has given us some confidence in extending the present macroscopic approach to superconductors.

The magnetic moment of the sample, associated with equilibrium currents $\mathbf{J}_S = -\mathrm{curl}\varepsilon$, is

$$\mathcal{M} = \tfrac{1}{2}\int \mathbf{r}\times\mathbf{J}_S d^3r = -\int \varepsilon d^3r + \oint \mathbf{r}\times(\varepsilon\times\mathbf{N}) d^2r \ , \quad (19)$$

then taking account of the boundary condition (15):

$$\mathcal{M} = -\int \varepsilon d^3r \ . \quad (20)$$

This relation clearly is a consequence of equilibrium equations (15) and (16), and $-\varepsilon$, no more than $\frac{1}{2}\mathbf{r}\times\mathbf{J}_S$, has the primary physical meaning of a magnetic moment density. It remains that a mean magnetization may be defined as $\mathbf{M} = \mathcal{M}/V$, where V is the sample volume. In cylinders, spheres, or slabs, $\mathbf{M} \simeq -\varepsilon_1$, the constant bulk value of ε; on the sample scale, diamagnetic currents are superficial, and give rise to the same field distribution as a uniform bulk magnetization, resulting in the same relationship between applied and bulk magnetic field: $\mathbf{B}_1 - \mathbf{B}_0 = \mu_0(1-D)\mathbf{M}$, where D is the demagnetizing factor.

Equations (14) and (16), together with $\nabla T = 0$, also characterize the absence of bulk dissipation, and should govern nondissipative transport currents through the vortex lattice. Consider a cylindrical sample, along the y direction, immersed in a transverse field $\mathbf{H}_0(0,0,H_0)$ as shown in Fig. 2(b). In the absence of flux flow, the total current through the cross section, expressed as a contour integral

$$I_1 = \int J_{Sy} dx\, dy = -\oint \varepsilon \cdot d\mathbf{l} \ , \quad (21)$$

is necessarily zero, by virtue of the surface condition $\varepsilon\times\mathbf{N} = 0$. We indeed find that a perfect sample has zero critical current, as it should be. A well-known exception to this rule arises, however, when $\mathbf{H}_0$ is directed parallel to planar faces of a prismatic sample. Vortex-free layers exist, at equilibrium, along a surface aligned with the field, the thickness of which also turns out to be of the order of d such as given above. This situation again is very similar to that observed in He II,[14] when cavity walls are aligned with the angular velocity. These vortex-free layers carry large supercurrents, which are responsible for the diamagnetism of the sample. But, as surface free-energy barriers are opposed to incoming or outgoing vortices, their thickness may be subject to significant deviations from equilibrium values; whereas symmetrical changes give rise to hysteresis, unsymmetrical changes can result in a net large transport current. Yet the occurrence of such supercooling or superheating effects in superconductors require a very good surface finish, in contrast with He II, where perfect plane walls on the scale of the vortex spacing ($a \sim 0,1$ mm) are easily obtained. On aligning the field $\mathbf{H}_0$ with carefully polished and annealed samples, a sharp maximum of I_c can be observed.[16] But this is not the case with samples of standard quality such as those used in the present work: polycrystalline square rods, spark machined, then chemically polished. Their critical currents were not very sensitive to field orientation (in the xz plane); a smooth maximum of I_c was observed with a relative variation $\Delta I_c/I_c$ not exceeding 20%. In all orientations critical currents usually are found to increase as the surface is roughened.[16] We presume, however, that the ability of the surface to carry transport supercurrents, when aligned with the field, should be first reduced, even though critical currents then increase by further roughening. Anyhow, the existence of any more or less rough faces, parallel to the field, will by no means alter the main conclusions, we wish to test by experiment, that in a soft material, on the scale of the sample, $I \leq I_c$ is superficial, and, in flux flow, VI_c is a surface Joule effect. Thus, while keeping in mind the peculiarity of a parallel surface, we shall simplify the discussion by assuming that the VL intersect the surface everywhere, as implied in expression (21) for the total nondissipative current I_1.

The continuum theory applies, and then the above results hold (in particular $I_1 = I_c = 0$) provided that the sample has no defects on the scale of the vortex spacing a. All thermodynamic local parameters, such as $H_c, \kappa, \varepsilon, \ldots$, if not uniform, must be slowly varying functions of position. If, moreover, the surface is smooth on the scale of a, the sample may be regarded as perfect, and $I_1 = I_c = 0$. Conversely, any departure from these ideal conditions is expected to be a source of pinning, in the sense that $I_c \neq 0$.

D. Surface critical currents

Hard samples such as sintered powders, industrial wires,... contain strong volume inhomogeneities like cavities, precipitates, ... In contrast, the samples used by experimentalists to test fundamental models, whether single crystals or rolled foils, generally are rather homogeneous, and indeed are designed for having well-defined characteristics ($\kappa, H_c, \varepsilon, \ldots$). However, bulk homogeneities does not prevent surface defects, and in most cases the roughness of the surface on a scale comparable to or smaller than a is unavoidable. PbBi or PbIn foils with a mirrorlike finish are obtained by compressing between glass plates; nevertheless, images provided by scanning tunneling microscopy reveal a very rugged surface

on the scale of a, bearing out the naive picture of Fig. 3.

As stated above, condition (17) holds on a microscopic scale (London model). Now, in the presence of surface irregularities on the scale of a, there should be many ways for the VL to end normal to the actual surface (Fig. 3), allowing for a large number of metastable or nondissipative solutions. This happens frequently in disordered systems, or in systems subject to irregular boundary conditions. Let us mention, for instance, the effect of surface roughness or heterogeneity on the wetability; surface heterogeneity permits the existence of many metastable configurations, and results in contact angle hysteresis.[17]

To take this feature into account, MS suggested[6] that the continuum description can be maintained, provided that the boundary condition be amended as follows: while still assuming idealized smoothed surfaces on the scale of a, condition (15) or (17) is released and replaced by an inequality in the form

$$(|\boldsymbol{\varepsilon}/\varepsilon\times\mathbf{N}| \text{ or } |\boldsymbol{\nu}\times\mathbf{N}| \leq \sin\theta_c \ , \tag{22}$$

where θ_c is a local critical angle increasing with the surface roughness (somewhat like a limiting friction angle in mechanics). When $\boldsymbol{\varepsilon}\times\mathbf{N}\neq 0$ in Eqs. (19) and (21), it is clear that the magnetic moment can differ from its ideal value (20) (hysteresis), and nondissipative transport currents can flow.

Consider the classical geometry of slabs or foils ($t \ll w$; Fig. 3), so as to work at low current densities, and $\boldsymbol{\varepsilon}\simeq\varepsilon\boldsymbol{\nu}$. Idealized faces are planes perpendicular to the applied field. In bending the VL near the surface in the direction indicated in the figure, as far as allowed by (22), a current density $\mathbf{J}_S=-\text{curl}\varepsilon\boldsymbol{\nu}$ will be systematically transported

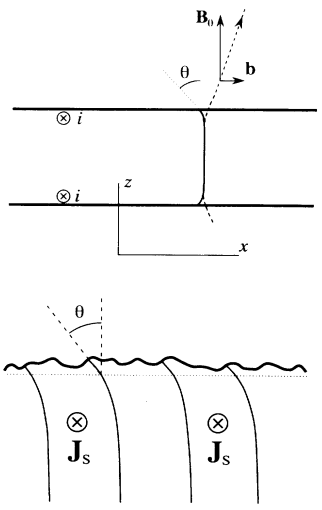

FIG. 3. Transport supercurrent in a foil normal to the magnetic field. Owing to surface irregularities on the scale of the vortex spacing, many metastable or nondissipative configurations of the vortex array should exist. Bending of vortices in the direction indicated in the figure makes the associated equilibrium currents J_S flow systematically in the y direction. As in Fig. 2, vortex lines in this perturbed layer are not flux lines, again in agreement with Eq. (3).

in the y direction, in accordance with Eq. (18). The same set of bulk equations entails again that the distortion of the vortex lattice and related equilibrium currents remain localized within a small depth d from the surface. Thus, integrating $\mathbf{J}_S$ over the depth d, we find the surface current density $i_y=-\varepsilon_x$, the surface component of $\boldsymbol{\varepsilon}$. Therefore, the local critical current density (A/m) is $i_c=\varepsilon\sin\theta_c$. Here ε strictly stands for its surface value, but if θ_c is not too large, ε is not very different from its bulk value $\varepsilon_1(B_1,T)$, where $B_1=B_0$. Hence, the critical current of a foil is predicted to be[3]

$$I_c\simeq 2w\varepsilon_1\langle\sin\theta_c\rangle \ , \tag{23}$$

where $\sin\theta_c$ has been averaged over the sample surface, and ε_1 is given as a function of H_0 and T by the fundamental equation of state (solid line in Fig. 1). Equation (23) involves two important results. First, it is seen that, with plausible values of $\sin\theta_c\sim 0.1$,[3] surface defects alone can account for the critical currents observed in soft samples. On the other hand, Eq. (23) asserts that the temperature and field dependence of I_c follows that of the vortex potential ε, a fact which is easily tested by experiment.[3] There is an obvious connection between critical currents and hysteresis, i.e., deviations from an ideal magnetization curve. However, this more indirect relationship between I_c and reversible magnetization itself (through ε), though sometimes noticed in the past,[1] is not often stated.

We wish to make a point in connection with Fig. 3. It should be noted that, because of the small field $\mathbf{b}$ due to the transport current $2i$, the flux lines are also slightly inclined to the normal, but in the opposite direction, with an angle of $b/B_0=i/H_0\sim\varepsilon\theta/H_0\ll\theta$. There is no inconsistency, having realized that $\boldsymbol{\omega}\neq\mathbf{B}$ in regions where $\text{curl}\mathbf{J}_S\neq 0$. In terms of forces, Eq. (16) means that the restoring force of bent vortices just offsets the mean Lorentz driving force. One cannot imagine such an equilibrium, as long as VL are believed to run along flux lines, since in this case both forces would act in the same direction.

One more point should be emphasized. No distinction has been made between diamagnetic currents and subcritical transport currents; both are nondissipative $\mathbf{J}_S=-\text{curl}\boldsymbol{\varepsilon}$ associated with the adequate distortion of the VL lattice, so that $\mathbf{C}=0$ in Eq. (16). In spite of their formal analogy, Eq. (16) and the familiar equation of magnetostatics, $\mathbf{J}_M=\text{curl}\mathbf{M}$, have quite different physical meanings. The former expresses an equilibrium, not the latter; $\mathbf{J}_M$ and curl$\mathbf{M}$ in a magnetic material are inseparable. Moreover, whereas $\mathbf{J}_S=-\text{curl}\boldsymbol{\varepsilon}$ may contribute to the transport currents, $\mathbf{J}_M$ never does.

E. Steady flux flow in a soft sample

For the sake of the discussion we shall consider a simple standard situation, in which the rod-shaped sample of Fig. 2 or 3 is assumed to have *uniform surface conditions* along its length, so that any segment Δy of the rod has the same critical current $[I_c(y)=\text{const}]$. We also assume *bulk homogeneity*. On the other hand, immersion of the

sample in superfluid He II ensures a *quasi-isothermal* process. Indeed small ∇T's arising from heat transfer cannot be ignored. Under these conditions, the V-I curve should display the standard broken shape: $V=0$ for $I<I_c$, and $V=R_f(I-I_c)$ for $I>I_c$. In practice, no sample is perfectly uniform. Each segment having a different critical current in a finite range, from I_c' to I_c'', the sum of individual linear characteristics result in a curved region of the overall V-I curve between I_c' and I_c''. The critical current usually obtained by extrapolating the linear part of the V-I curve is then interpreted as the mean value of $I_c(y)$ between the voltage probes.[18]

According to experiment, macroscopic space charges, Bernoulli and Hall effects are negligibly small, so that $\bar{\mu}=$const in the homogeneous rod, and $\mathbf{E}'=\mathbf{E}(0,E,0)$ is longitudinal. Moreover, stationary conditions require $\mathbf{E}$ to be uniform everywhere inside the sample. Recall that no induced voltage can exist in steady flux flow, as far as macroscope fields are concerned.[19] We believe that this uniform electric field is due to minute electrostatic charges distributed, thanks to the generator, on the sample surface, just as it is in any conducting wire, or in the normal state, without discontinuity across H_{c2}. Note that the classical relationship between the macroscopic electric field and the VL velocity $\mathbf{v}_L$ (Ref. 19) is recovered in the MS theory as a consequence of conservation laws; from its generalized form, $\mathbf{E}'=-\mathbf{v}_L\times\boldsymbol{\omega}$ [see Eq. (39) below], where $\mathbf{E}'\neq\mathbf{E}$ and $\boldsymbol{\omega}\neq\mathbf{B}$, it is clear that it does not express the law of induction.

A picture of the dc flux flow in a soft sample follows at once from the above interpretation of surface pinning. The observed shape of the V-I curve suggests that the surface retains its ability to carry a constant nondissipative current, $I_1=I_c$ (i.e., its maximum value as much as allowed by surface defects), while the voltage V across the sample should be proportional to the dissipative excess current, $I_2=I-I_1=V/R_f$. Accordingly, it is convenient to separate the local current density $\mathbf{J}$ into two parts:

$$\mathbf{J}=\mathbf{J}_1+\mathbf{J}_2=-\mathrm{curl}\varepsilon+\mathbf{J}_2\ . \tag{24}$$

$\mathbf{J}_1=-\mathrm{curl}\varepsilon$ is defined, at any point and time, as the supercurrent (including diamagnetic currents) that would come into equilibrium with the vortex array in its instantaneous configuration; it should represent the nondissipative part of the supercurrent. The "core" current $\mathbf{C}=\mathbf{J}_S-\mathbf{J}_1$ is its dissipative part. Thus, we can *define* the critical current, in the flux-flow regime, as the integral sum of $\mathbf{J}_1$ over the cross section such as given by Eq. (21). As $I_2\propto V$ and $\mathbf{E}=$const we expect that $\mathbf{J}_2=\sigma_f\mathbf{E}$ (σ_f is the flux-flow conductivity) and is uniformly distributed in the bulk, whereas currents $\mathbf{J}_1$ remain localized near the sample surface. Therefore, the experimental shape of the V-I curve is well explained, if the vortex array is assumed to move uniformly while maintaining its critical state configuration, as sketched in Fig. 4. We are fully aware that the rigid and uniform motion of VL, especially near the surface, is unrealistic. But we regard it as a time-average picture of the vortex flow, which will be useful for dealing with dc transport properties. Actually, the

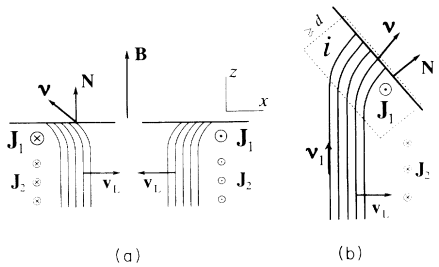

FIG. 4. A time-average picture of the vortex flow: (a) near a face normal to the field, for both directions of the dc current; (b) near a face inclined to the field. The transport theory brings out the existence of an important convective term in the energy flux, denoted as $\boldsymbol{\varepsilon}\times\boldsymbol{\varphi}\simeq\varepsilon\mathbf{E}\times\boldsymbol{\nu}$ in the text [see Eq. (35)]; in any case its surface component is pointing outwards and contributes to the heat ejected to the surrounding bath. Thus, it accounts for a large part of the Joule effect, as explained in Sec. III. In perfect samples, vortices would end normal to the boundary ($\boldsymbol{\nu}=\mathbf{N}$), and this surface Joule effect would vanish.

motion of VL slipping through the surface defects must be irregular, giving rise to large local fluctuations of the VL bending and associated $\mathbf{J}_1$'s (flux-flow noise). Nevertheless, the relative fluctuations δI_1 of the critical current I_1 (the sum of statistically independent $\delta\mathbf{J}_1$'s) are considerably reduced by a well-known statistical effect, to typically 10^{-3}–10^{-4}. At constant I, correlative fluctuations $\delta I_2=-\delta I_1$ entail a small voltage noise. Pursuing this idea, a consistent theory of flux-flow noise, supported by experiments, has been proposed recently,[12] and is planned to be published elsewhere. Though detectable,[20] the resulting fluctuations of the Joule effect are negligibly small. In many respects, therefore, the effects of flux-flow noise may be ignored. Thus, we shall adopt the point of view that all quantities of interest in a dc problem can be calculated with a good approximation by using the time averages of the fields, which amounts to handling the time-average vortex flow, as if it were strictly steady. This is a familiar procedure in the hydrodynamics of turbulence; in many practical situations, only the mean flow development is of real interest. The structure of the "turbulence" of the vortex flow should be relevant only in so far as it determines voltage noise.

It must be admitted that such an assumption is by no means obvious; concerning dissipative quadratic terms (e.g., $\propto v_L^2$), it implies that the statistical dispersion of the fields (e.g., the time average of δv_L^2) is not significant. In contrast, the current theories of pinning introduce elastic instabilities at the pinning sites involving a large dispersion of v_L, with the main purpose of accounting for the part VI_c of the Joule effect.

In this connection, one objection could have been raised to our interpretation from the beginning. In steady conditions, the work supplied by the generator, $VI=VI_1+VI_2$, is completely transformed into heat delivered into heat reservoir. From this, one generally infers that I_1 should also contribute to dissipation, at variance with the stated property of the currents $\mathbf{J}_1$. As

discussed in Sec. III, there is no inconsistency, however, and a careful analysis of the Joule effect in the mixed state corroborates the foregoing considerations.

III. THE JOULE EFFECT IN THE MIXED STATE

A. General transport equations

Once one accepts the thermodynamic identity (8) and the bulk equilibrium equations, $\nabla T=0$, $\mathbf{E}'=0$, and $\mathbf{C}=0$, a consistent set of transport equations is easily derived[6] repeating a rigorous standard method.[7] Let us write the laws of energy conservation and entropy growth in their general form

$$\frac{\partial \overline{U}}{\partial t}+\mathrm{div}\mathbf{J}_U=0 , \tag{25}$$

$$\frac{\partial \overline{\sigma}}{\partial t}+\mathrm{div}\frac{\mathbf{Q}}{T}=\frac{R}{T} , \tag{26}$$

in which $\mathbf{J}_U$, $\mathbf{Q}$, and $\mathbf{Q}/T$ are current densities of energy, heat, and entropy, respectively. Taking the left-hand sides of the equilibrium conditions, namely, ∇T, $\mathbf{E}'$, and $\mathbf{C}$, as affinities, we expect the dissipative function R to be expressed as the sum of products of each affinity with an associated flux to be determined. Expressing $\partial \overline{U}/\partial t$ from Eq. (8), and substituting the time derivatives from Eqs. (3), (26), and Maxwell equations, then comparing with Eq. (26), we obtain

$$R=-\frac{\mathbf{Q}}{T}\cdot\nabla T+\mathbf{J}_n\cdot\mathbf{E}'-\boldsymbol{\varphi}\cdot\mathbf{C} , \tag{27}$$

$$\mathbf{J}_U=\mathbf{Q}-\frac{\mu}{e}\mathbf{J}+\mathbf{S}+\boldsymbol{\varepsilon}\times\boldsymbol{\varphi} . \tag{28}$$

Here $\mathbf{J}$ is the total current density (the charge flux). $\mathbf{J}_n$ stands for $\mathbf{J}-\mathbf{J}_S$ and may be referred to as the normal current. $\mathbf{S}=\mathbf{E}\times\mathbf{B}/\mu_0$ is the Poynting vector, and $\boldsymbol{\varphi}$ is defined by

$$-\frac{m}{e}\frac{\partial \mathbf{v}_S}{\partial t}=\mathbf{E}'+\boldsymbol{\varphi} . \tag{29}$$

Equation (29) reads as the macroscopic equation of motion of the supercurrent, in a form generalizing the second London equation. The "force" field $\boldsymbol{\varphi}$ is the analogue of the mutual friction force in He II.[7]

The heat balance equation can be rewritten in the simplified form

$$T\frac{\partial \overline{\sigma}}{\partial t}+\mathrm{div}\mathbf{Q}=g=\mathbf{J}_n\cdot\mathbf{E}'-\boldsymbol{\varphi}\cdot\mathbf{C} , \tag{30}$$

where g ($\mathrm{W/m^3}$) is the local heat source due to dissipation (bulk Joule effect).

Let us for a moment assume that each flux, as generally observed, depends only on its own associated affinity. Just as in He II, the linear law $-\boldsymbol{\varphi}\propto\mathbf{C}$ can be written as $-\varphi_i=\omega\beta_{ik}C_k$ by introducing the friction tensor β_{ik}. By symmetry arguments this tensor has only three independent components; in vectorial form[7]

$$-\boldsymbol{\varphi}=\beta\omega\mathbf{C}_\perp+\beta'\omega(\boldsymbol{\nu}\times\mathbf{C})+\beta''\omega\mathbf{C}_\parallel ,$$

where $\mathbf{C}_\perp=(\boldsymbol{\nu}\times\mathbf{C})\times\boldsymbol{\nu}$ and $\mathbf{C}_\parallel=(\boldsymbol{\nu}\cdot\mathbf{C})\boldsymbol{\nu}$. Since $R>0$, β and β'' are positive coefficients. The law of thermal conductivity, $Q_i=\kappa_{ik}\nabla_k T$, and the law of electrical conductivity of the "normal fluid," $J_{ni}=\gamma_{ik}E'_k$, can be written in the same form. In the absence of significant Hall effects (electrical or thermal), the associated descriptive coefficients, β', κ', and γ' may be neglected. Furthermore, as already pointed out for He II,[7] the conservation of VL should imply that $\beta''=0$. Indeed, if $\beta''=0$, $\boldsymbol{\varphi}$ takes the form $\mathbf{v}_L\times\boldsymbol{\omega}$. Taking the curl of Eq. (29), we obtain

$$\frac{\partial \boldsymbol{\omega}}{\partial t}=\mathrm{curl}\boldsymbol{\varphi}=\mathrm{curl}\mathbf{v}_L\times\boldsymbol{\omega} ,$$

which reads as a transport equation for vortices, with the line velocity $\mathbf{v}_L$. The simplified linear laws are

$$\mathbf{Q}=-\kappa\nabla T_\perp-\kappa''\nabla T_\parallel , \tag{31}$$

$$\mathbf{J}_n=\gamma\mathbf{E}'_\perp+\gamma''\mathbf{E}'_\parallel , \tag{32}$$

$$\boldsymbol{\varphi}=-\beta\omega\mathbf{C}_\perp=\mathbf{v}_L\times\boldsymbol{\omega} , \tag{33}$$

$$\mathbf{v}_L=-\beta\boldsymbol{\nu}\times\mathbf{C} . \tag{34}$$

Having defined $\mathbf{v}_L$ as a vector normal to VL (and assuming $\boldsymbol{\varepsilon}\simeq\varepsilon\boldsymbol{\nu}$) the last term in $\mathbf{J}_U$ can be looked on as a transfer of energy by convection:

$$\boldsymbol{\varepsilon}\times\boldsymbol{\varphi}\simeq\varepsilon\boldsymbol{\nu}\times\boldsymbol{\varphi}=\varepsilon(\omega)\omega\mathbf{v}_L . \tag{35}$$

B. Thermomagnetic effects

In writing the foregoing dynamical equations, we have deliberately left out cross terms. However, we cannot ignore the considerable heat current $\mathbf{q}_L$ associated with vortex motion,[21,22] which gives rise to an abnormally large Ettingshausen effect in a type-II superconductor as compared with a normal metal. To take this into account, a second term $\mathbf{q}_L\propto\mathbf{C}$ should be added in Eq. (31), for instance, in the form $-AT(\boldsymbol{\omega}\times\mathbf{C})$, as well as the term $A(\boldsymbol{\omega}\times\nabla T)$ in Eq. (33), in accordance with Onsager reciprocity:

$$\mathbf{Q}=\mathbf{q}+\mathbf{q}_L=\mathbf{q}-AT(\boldsymbol{\omega}\times\mathbf{C}) , \tag{36}$$

$$\boldsymbol{\varphi}=-\beta\omega\mathbf{C}_\perp+A(\boldsymbol{\omega}\times\nabla T) . \tag{37}$$

Here $\mathbf{q}$ stands for the heat current due to thermal conduction [the right-hand side of Eq. (31)].

In experiments we shall ascertain that ∇T's resulting from both Joule and Ettingshausen effects remain small enough, so that no related effect, except for $\mathbf{q}$ itself, is significant; the temperature dependence of kinetic coefficients, as also the "thermal force" in Eq. (37) (or any term $\propto A\nabla T$) are negligible secondary effects. That is just what we mean above by *quasi-isothermal process.* Under these conditions, $\mathbf{q}_L$ can be rewritten as a convective flux. Equations (33) and (34) yield

$$\mathbf{q}_L=\frac{AT}{\beta}\omega\mathbf{v}_L=nTS_d\mathbf{v}_L , \tag{38}$$

where $S_d=A\varphi_0/\beta$ is commonly known as the transport entropy per vortex.[21]

C. Steady flux flow

Under stationary conditions, Eq. (29) reads

$$\mathbf{E}' = -\boldsymbol{\varphi} = -\mathbf{v}_L \times \boldsymbol{\omega} \ . \tag{39}$$

This becomes the well-known relationship between $\mathbf{E}'$, $\mathbf{v}_L$, and $\mathbf{B}$,[19] where supercurrents are evenly distributed, so that $(m/e)\mathrm{curl}\mathbf{V}_S \ll \mathbf{B}$ and $\boldsymbol{\omega} \simeq \mathbf{B}$, i.e., in general, in the bulk of the sample. Equation (39) holds under *quasi-stationary conditions* as far as one can neglect the inertial term in Eq. (29) compared to $\mathbf{E}$. It is a very good approximation for ac currents in the acoustic range of frequencies, and over the whole spectrum of flux-flow noise (0–1 kHz).

The heat source g then becomes

$$g = \mathbf{E}' \cdot (\mathbf{J}_n + \mathbf{C}) = \mathbf{E}' \cdot \mathbf{J}_2 \ , \tag{40}$$

where $\mathbf{J}_2$ has been defined in Sec. II as the dissipative part of the current; from Eq. (24),

$$\mathbf{J}_2 = \mathbf{J} - \mathbf{J}_1 = \mathbf{J} + \mathrm{curl}\boldsymbol{\varepsilon} = \mathbf{J}_n + \mathbf{J}_S + \mathrm{curl}\boldsymbol{\varepsilon} = \mathbf{J}_n + \mathbf{C} \ . \tag{41}$$

To some extent, no distinction being made between ω and $\mathbf{B}$, nor between $\mathbf{E}'$ and $-\boldsymbol{\varphi}$, the formalism worked out in the foregoing transport equations was available before, in previous analyses of dissipation.[1,10] Hu's expression for $\mathbf{J}_U$ and R (Ref. 10) can be identified with ours in the stationary case, provided that $-\boldsymbol{\varepsilon}$ and $\mathbf{J}_2$ should be substituted to $\mathbf{M}$ and $\mathbf{J}_t$. The term $\boldsymbol{\varepsilon} \times \boldsymbol{\varphi}$ has been introduced in the form $\mathbf{M} \times \mathbf{E}'$ as a correcting term in $\mathbf{J}_U$.[10,22] As discussed in Sec. II with regard to magnetization, all the difference lies in the interpretation of the quantities involved. In Refs. 1 and 10 the current $\mathbf{J}_t$ entering into the dissipative function, as $\mathbf{E} \cdot \mathbf{J}_t$, is always termed the *transport current density*. This leads the authors to the conceptual division of $\mathbf{J}$ into a transport current and a magnetization current, $\mathbf{J} = \mathbf{J}_t + \mathbf{J}_m$. Our point of view is quite different, since the dissipative current $\mathbf{J}_2$ in Eq. (40) is *only a part* of the transport current (except for perfect samples). We have seen how, in the presence of defects, $\mathbf{J}_1$ may contribute largely to the total transport current, while being locally indistinguishable from diamagnetic currents.

Let us return to the standard stationary situation such as described above and illustrated in Fig. 4. As stated at the end of Sec. II, we restrict ourselves to investigating the time-average vortex flow, which is steady and two-dimensional in the mean, the VL lying in x-z planes and all currents being along y, as shown in Fig. 4. Thus, $\mathbf{E}' = \mathbf{E} = \beta\omega\mathbf{C} = \mathrm{const}$, $\mathbf{J}_n = \gamma\mathbf{E} = \mathrm{const}$. In the bulk, moreover, beyond the perturbed depth d, $\boldsymbol{\omega} \simeq \mathbf{B}$, $\mathbf{J}_1 \simeq 0$, $\mathbf{J}_2 \simeq \mathrm{const}$, and the heat sources g are uniformly distributed. From Eqs. (32) and (33), it follows that

$$\mathbf{J}_2 = \left[\gamma + \frac{1}{\beta\omega}\right]\mathbf{E} = \sigma_f \mathbf{E} \ . \tag{42}$$

For instance, the flux-flow conductivity σ_f derived by Schmid, [11] close to H_{c2}, may be written in the form (42), by taking $\omega = B$, $\gamma = \sigma_n$, the normal conductivity, and $\beta = \xi^2/2\tau\varepsilon$, where τ is defined by Eq. (5) and ε is given by Eq. (11).

We now turn our attention to the *heat transfer* from the sample to the heat reservoir at T_0. The sample is immersed in an electrically insulating bath, which, in general, obeys a simpler set of transport equations. In an ordinary electrical insulator, heat and energy fluxes can be identified, except for the Poynting vector, $\mathbf{J}'_U = \mathbf{q}' + \mathbf{S}'$ (primed quantities will relate to the surrounding medium). This holds in superfluid helium, where $\mathbf{q}' \simeq T_0 \sigma' \mathbf{v}'_n$ ($\mathbf{v}'_n$ is the normal fluid velocity), and, of course, in vacuum with $\mathbf{q}' = 0$. In any case one must be careful in writing the boundary condition for heat flow at the interface; it is obtained by equating the normal components of *energy fluxes*, $\mathbf{J}_U \cdot \mathbf{N} = \mathbf{J}'_U \cdot \mathbf{N}$. Since $\mathbf{J} \cdot \mathbf{N} = 0$, and $\mathbf{S} \cdot \mathbf{N} = \mathbf{S}' \cdot \mathbf{N}$, because of the continuity of the fields (the normal component of the electrical field excepted), we find

$$q'_N = Q_N + (\boldsymbol{\varepsilon} \times \boldsymbol{\varphi}) \cdot \mathbf{N} = Q_N + h \ , \tag{43}$$

where

$$h = (\boldsymbol{\varepsilon} \times \mathbf{N}) \cdot \boldsymbol{\varphi} = -\varepsilon_T E \ . \tag{44}$$

Here, subscripts N and T denote outward normal and clockwise tangential components, respectively. The net outward flux of heat, per unit length along y, is the surface integral of q'_N. It appears as the sum of two terms. According to Eq. (30), the surface integral of Q_N is just the volume integral of g, i.e., EI_2. Then, using Eq. (21), the second term can be rewritten as

$$\oint h \, dl = -E \oint \boldsymbol{\varepsilon} \cdot d\mathbf{l} = EI_1 \ , \tag{45}$$

which is the expected remaining part of the total Joule effect EI. In solving the whole set of heat equations, it will be convenient to regard heat as being conserved, provided that the term $\mathbf{h}$ ($\mathrm{W/m^2}$) is taken into account as a *surface heat source*.

Figure 4(a) represents the mean vortex flow near a face normal to the field, for both directions of the applied current. Because of the steady bending of VL, the energy flux $\boldsymbol{\varepsilon} \times \boldsymbol{\varphi}$ has a component normal to the boundary, which is responsible for the surface Joule effect. Despite the fact that $\boldsymbol{\varepsilon} \times \boldsymbol{\varphi} = \mathbf{E} \times \boldsymbol{\varepsilon}$ can be identified in the bulk as an odd effect, changing sign with I (or $\mathbf{B}$), the energy current at the interface is always seen to be outward ($\mathbf{h} > 0$), as expected for an even Joule effect. Moreover, the surface Joule effect is the only way of revealing the energy flux $\boldsymbol{\varepsilon} \times \boldsymbol{\varphi}$: consider the case shown in Fig. 4(b), where, inversely, the curvature of VL prevents the bulk energy flux $\mathbf{E} \times \varepsilon_1 = \varepsilon_1 \omega_1 \mathbf{v}_L$ from reaching the surface. As a matter of fact, such a large odd effect is not observed, but this is not explained by the authors[22] except for stating the wrong boundary condition $Q_N = 0$ at the sample-vacuum interface, instead of the right one $J_{UN} - S_N = 0$. As easily seen, the conservation of the energy flux through the curved vortex array is ensured by a correlative abrupt change in the Poynting flux: consider a thin flat box enclosing the perturbed layer, of area $dl \times 1$ and thickness $\gtrsim d$, as indicated in Fig. 4(b). Let $\mathbf{q}_1, \mathbf{S}_1, \ldots$ be the fluxes at the inner face of the box; except for $\mathbf{q}_1(\mathbf{r})$, these are the quasiuniform bulk values of $\mathbf{q}_L$, $\mathbf{S}$, $\boldsymbol{\varepsilon} \times \boldsymbol{\varphi}$.

Again, the energy conservation requires that

$$S'_N+q'_N=S_{1N}+Q_{1N}-E\varepsilon_{1T} .$$

According to Poynting equation, $S_{1N}-S'_N=Ei$, where $i=i_1+i_2\simeq i_1=\varepsilon_{1T}-\varepsilon_T$ ($\mathbf{J}_1=-\mathrm{curl}\boldsymbol{\varepsilon}$); whence

$$q'_N=Q_{1N}+Ei_2+E(i_1-\varepsilon_{1T})\simeq Q_{1N}+h . \quad (46)$$

As $Q_N=Q_{1N}+Ei_2\simeq Q_{1N}$ (by Eq. (30)], we return to Eqs. (43) and (44), as it should. This alternative derivation of the boundary conditions for the heat flow can be readily extended to cases where $\mathbf{H}_0$ is aligned with a face of the sample. In any case, $i_c=i_1-\varepsilon_{1T}$ may be defined as the local contribution to the critical current.

Assuming dc or very low-frequency currents, and quasi-isothermal conditions, the term $\mathrm{div}\mathbf{q}_L$ in Eq. (30) vanishes in the bulk. Allowing for possible thermal inertial effects, and setting $Td\bar{\sigma}\simeq cdT$, where c is the specific heat (in J/m^3 K), the bulk heat equation finally reduces to

$$c\frac{\partial T}{\partial t}+\mathrm{div}\mathbf{q}=g=\mathrm{const} , \quad (47)$$

where $\mathbf{q}$ is subject by Eq. (46) to the boundary conditions

$$q'_N=q_{1N}+h_L+h \quad (h_L=\mathbf{q}_{L1}\cdot\mathbf{N}) . \quad (48)$$

Equivalently stated, the Ettingshausen effect may be treated, on the scale of the sample, as anoher *surface heat source* h_L (actually distributed over a small depth of the order of d). Given the sources g, h, and h_L, the problem of heat transfer will be entirely specified by an additional condition on q'_N, depending on the embedding medium. In He II, q'_N can be expressed in terms of the temperature T and T' at the interface as

$$q'_N=\frac{T-T'}{R_K} \quad (T'\simeq T_0) , \quad (49)$$

where R_K (~ 1 K cm^2/W) is the Kapitza resistance. This is illustrated in Fig. 5 by the one-dimensional electric analogue of a sample He II interface.

A last observation should be made concerning the formalism. If one desired to introduce a *local* $\mathbf{H}$ *field,* a possible definition would be $\mathbf{H}=\mathbf{B}/\mu_0+\boldsymbol{\varepsilon}$, which is closest to previous definitions.[1,9] So the fluxes $\mathbf{S}$ and $\mathbf{E}\times\boldsymbol{\varepsilon}$ could be cast in one new vector $\mathbf{S}^*=\mathbf{E}\times\mathbf{H}$. However, one should renounce properties customarily attached in magnetism to a vector $\mathbf{H}$: here, $\mathrm{curl}\mathbf{H}=\mathbf{J}-\mathbf{J}_1=\mathbf{J}_2$ is *not* the transport current, and the parallel component of $\mathbf{H}$ at the interface is no longer continuous, nor is S^*_N.

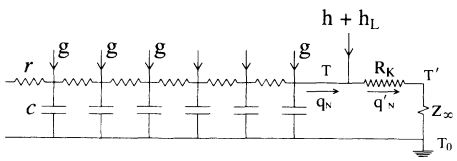

FIG. 5. The one-dimensional electrical analogue of a unit area of sample He II interface. Current and voltage along the r-c line are the analogues of $q=-\kappa\nabla T$ and T. Here $r=\kappa^{-1}$, c is the specific heat, R_K is the Kapitza resistance, and $z_\infty \ll R_K$ the bulk He II impedance. The problem of heat transfer becomes one dimensional when the thermal skin depth $\delta=(rc\omega/2)^{-1/2}$ is small compared to the sample size.

IV. SECOND-SOUND EXPERIMENT

The samples used were square rods of cross section 4×4 mm^2, spark cut from PbIn 17.5 at. % polycrystalline ingots. Critical currents, typically $I_c\sim 10$ A at $H_0=0.5H_{c2}$, may seem to be low to one accustomed to expressing them in terms of critical current density J_c. However, foils rolled from the same ingots had similar critical currents. Various sample treatments—annealing, chemical polishing, plating—could affect I_c, but did not alter the qualitative results such as described in this section.

Complete immersion in superfluid helium, at $T_0=1.66$ K, allowed us to use high currents, while still satisfying quasi-isothermal conditions, in the sense given in Sec. III. Consider, for example, the working conditions reported in Figs. 6–8: at $B_0=3000$ G ($B_{c2}=4770$ G), up to $I\simeq 20$ A, ΔT's arising throughout the sample because of the g sources do not exceed 0.1 K; with $\beta\omega\sim\rho_f\sim 10^{-7}$ Ω m (Fig. 6) and $S_d\sim 10^{-13}$–10^{-12} J/m K, the thermal forces in Eq. (37) stay small as compared with E. The temperature jump $T-T'$, at the interface, is of the order of a few mK.

The sample is driven by a modulated current, $I+I^*e^{j\omega t}$, where $I^*\lesssim 0.5$ A. At $I^*=$const, the operating point (I,V) is moved along the linear part of the V-I curve. The frequency ω is low enough to ensure a *quasi-static modulation* of the dc characteristic, as carefully checked experimentally. The g and h sources are modulated accordingly, all being in phase with the applied current. Below, an asterisk will designate the ω components of fields, sources, and fluxes. The resulting heat

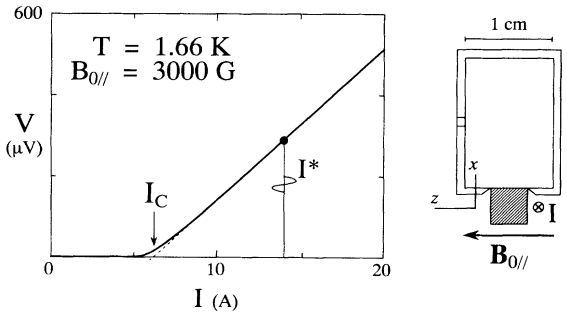

FIG. 6. A schematic of the fitting of a PbIn square rod on a rectangular second-sound resonator. Also shown is the measured dc voltage-current characteristic at 1.66 K, $B_{0\|}=3000$ G ($I_c=6.2$ A); the solid dot indicates the operating point for data reported in Fig. 7. A small superimposed ac current ($I^*\simeq 0.7$ A) modulates Joule and thermomagnetic heat sources. The sample acts as a second-sound transmitter and drives the cavity on its x fundamental mode, $\omega_0/2\pi\simeq 640$ Hz, at 1.66 K (quality factor 1650). A carbon bolometer (not shown) measures both amplitude and phase of the temperature oscillations. Its response (typically $\sim 10\,\mu$V) is amplified and directly plotted on the Argand plane, as shown in Fig. 7.

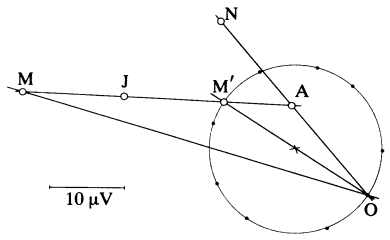

FIG. 7. Typical X-Y recording of the complex amplitude s of the second-sound signal. Solid points are experimental points for a set of discrete values of ω close to the fundamental resonant frequency ($\omega_0/2\pi \simeq 640$ Hz, at 1.66 K). The response curve $s(\omega)$ is a circle from which the theoretical resonant signal $s(\omega_0)$ is deduced accurately. This graphical construction allows one to get rid of resonance shifts due to possible temperature drift during the experiment. $\mathbf{s}(\omega_0)=OM$ refers to the working conditions shown in Fig. 6 ($I=14$ A). OM' is obtained on reversing the direction of the magnetic field. The even part of s is the Joule signal OJ. As explained in the text, the signal in the normal state, ON ($I \lesssim 5$ A, $I^* \sim 0.5$ A), and the odd thermomagnetic signal JM yield phase references for volume and surface heat sources, respectively. Thus, OJ is resolved into components, as $OA+AJ=\mathbf{s}_1+\mathbf{s}_2$ ascribed to volume and surface Joule effects, respectively.

flow at the interface $q'_N e^{j\omega t}$ generates second-sound waves around the sample, which therefore acts as a second-sound transmitter. The working frequency ω matches the fundamental mode ω_0 of a rectangular resonator, a wall of which is closed by one face of the sample as shown in Fig. 6. Thus, the cavity selectively amplifies second sound issuing from this face. At 1.66 K, $\omega_0/2\pi=640$ Hz. The magnetic field can be rotated to be either aligned with (Fig. 6) or perpendicular to the transmitting face (in short notation $H_{0\parallel}$ or $H_{0\perp}$).

The cavity is machined from epoxy resin rods and carefully bonded with an epoxy adhesive. A slit at the midheight of the cavity allows helium to flow inside and the dc heat to escape. Since R_K is large as compared with the characteristic impedance of bulk He II ($z_\infty \sim 10^{-3}$ K cm^2/W), the sample behaves as a quasiperfect second-sound reflector, like other walls. A carbon bolometer painted on the opposite wall measures the temperature amplitude *and phase* of the second-sound standing wave. The bolometer signal s is fed into a two-phase

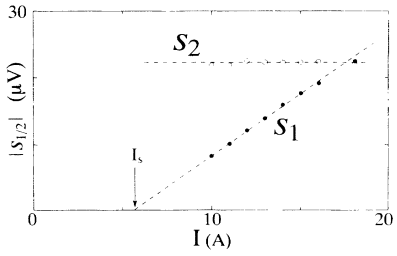

FIG. 8. The magnitude of the Joule components of the second-sound signal, s_1 and s_2 as function of the dc applied current. Data are taken along the V-I curve of Fig. 6.

lockin amplifier, whose outputs drive an XY recorder. Thus, the second-sound signal is directly plotted as a vector s in the Argand plane (Fig. 7). s is proportional to the ω component of the heat input q'_N, averaged over the transmitting face: $s=\mathcal{A}(\omega)\langle q'^*_N \rangle$, where $\mathcal{A}(\omega)$ is the overall transfer function of the cavity-bolometer system. In the plot of Fig. 7, $\mathcal{A}(\omega_0)$ at the resonance may be regarded as an arbitrary complex factor. Nevertheless, some cavities have been calibrated by using a thin chromium film as an auxiliary transmitter; when driven at $\frac{1}{2}\omega$, such a film delivered a known heat current (at ω) into the cavity.

This second-sound technique has long been proposed by one of us and developed by Vidal[23,24] as an alternative way of measuring thermomagnetic effects. In these pioneering experiments, the whole current I was modulated, eliminating the ω component of Joule sources. But the nonlinear response of the sample, and spurious couplings between the cavity and the external bath, made the analysis of the results delicate. Since then, we have made considerable progress in second-sound acoustics[14,20] which might renew the metrological interest of this method. But we are not concerned here in measuring S_d, and the reported experiment has been designed merely to be demonstrative. Note, however, the great convenience of the Ettingshausen effect, inasmuch as it behaves as surface heat sources and provides us a useful reference signal. The ω component of the Ettingshausen equivalent sources are $h_L^*=\pm E^* T S_d/\varphi_0$ on faces aligned with $\mathbf{H}_0$ and zero elsewhere.

The ω component of the total Joule effect, irrespective of any model, reads

$$VI^*+V^*I=V^*I_c+2V^*(I-I_c)\ ,$$

where $V^*=R_f I^*$. Now, in ideally soft samples (no volume pinning), we expect V^*I_c to be distributed as surface sources $h^*=E^* i_c$, while $2V^*(I-I_c)$ should be uniformly distributed in the bulk as g^* sources; $g^*=2E^* J_2$.

As has been remarked above, no electrical skin effect can be detected in the working frequency range. In contrast, *thermal inertial effects* are important. Referring, for instance, to the normal state at 1.66 K ($\kappa_n=0.49$ W/m K, $c_n=8.25\times 10^2$ J/m^3 K), the thermal skin depth at 640 Hz is $\delta_n=(2\kappa_n/c_n\omega)^{1/2}=0.54$ mm. Therefore, the cavity only captures the heat sources in the immediate vicinity of the transmitting face. As a first and fairly good approximation, a one-dimensional calculation (see Fig. 5) yields

$$q'^*_N=\alpha\left[\frac{g^*\delta}{1+j}+h^*+h_L^*\right]\ . \tag{50}$$

Here $\delta=(2\kappa/c\omega)^{1/2}\sim\delta_n$ is the thermal skin depth (assuming for simplicity $\kappa\simeq\kappa''$), and $\alpha=[1+(1+j)\eta]^{-1}$, where $\eta=\kappa R_K/\delta\sim 0.1$. Equation (50) accounts for the main features of experimental results.

Let $\mathbf{s}_1$, $\mathbf{s}_2$, and $\mathbf{s}_3$ be the signals due, respectively, to sources g^*, h^*, and h_L^* taken separately. The resulting signal $\mathbf{s}=\mathbf{s}_1+\mathbf{s}_2+\mathbf{s}_3$, at $\omega=\omega_0$, is recorded in the complex plane as a function of I and B_0 (Fig. 7), while maintaining

a constant modulation E^* (or V^* or I^*). On reversing the magnetic field (or I), only $\mathbf{s}_3$ change sign. From $\mathbf{s}(\mathbf{H}_0)=\mathbf{OM}$ and $\mathbf{s}(-\mathbf{H}_0)=\mathbf{OM}'$, we get $\mathbf{M}'\mathbf{M}=2\mathbf{s}_3$, and the Joule signal even in $\mathbf{B}_0$, $\mathbf{OJ}=\frac{1}{2}(\mathbf{OM}+\mathbf{OM}')$. For $\mathbf{H}_{0\perp}$, $\mathbf{OM}=\mathbf{OM}'$, within the precision of the recorder pen ($\mathbf{s}_3=0$). In Fig. 7, the signal $\mathbf{s}(\mathbf{H}_0)=\mathbf{OM}$ has been obtained in $\mathbf{H}_{0\parallel}$ for directions of $\mathbf{H}_0$ and I such as $h_L>0$ on the transmitting face. So the direction of the axis $M'M$ gives the phase of the signal $\mathbf{s}_2$ that would result from the modulation of h sources *flowing inwards* ($h>0$); upon increasing B_0 from 2000 to 4500 G, we observed no significant change ($\lesssim 2°$) of this phase. This is consistent with the fact that, according to Eq. (50), the phase of $\mathbf{s}_3$ follows that of the factor α, which at any rate is close to unity. Possible variations of involved parameters R_K, κ, and c, only affect the small term $\eta\sim 0.1$. If $\alpha\simeq$const, the phase of a signal $\mathbf{s}_1$, due to uniform volume sources, is given by the Joule signal in the normal state, $\mathbf{s}_n=\mathbf{OM}_n$. We verify that $\mathbf{s}_n$ lags $\mathbf{s}_3$ in phase by an angle near $\pi/4$, such as predicted by the one-dimensional (1D) formula (50).

The drawing of Fig. 7 is repeated for various values of I along the linear part of the V-I curve. It is noticed at once that the Joule point J moves parallel to the axis OM_n. Therefore, the simplest way of describing the I dependence of the Joule signal is to resolve $\mathbf{OJ}$ into two components, $\mathbf{s}_1$ and $\mathbf{s}_2$, along the axes OM_n and $M'M$. Then the magnitude of $\mathbf{s}_1$ and $\mathbf{s}_2$ is plotted as function of I (Fig. 8). It is found that s_1 increases linearly as $I-I_s$, with $I_s\simeq I_c$, while s_2 is nearly constant; that is, the expected behavior of the sources $g^*=2E^*J_2$ and $h^*=E^*i_c$ (at $E^*=$const). The simplicity of this result justifies ascribing the signal s_2 so defined to the surface Joule effect.

To confirm the connection between the $\mathbf{s}_2$ component and the critical current, we have measured s_2 and I_c as function of B_0, from 2000 to 4500 G. While I_c is reduced by a factor 5, the ratio s_2/I_c is found remarkably constant (to better than 2%). On the other hand, absolute measurements of $\langle h^*\rangle$, averaged over the transmitting face, could be obtained from s_2 in calibrated cavities (see above). By $\langle h^*\rangle=E^*\langle i_c\rangle$, the contribution to I_c of this face was calculated, for both orientations of the field $\mathbf{H}_{0\parallel}$ and $\mathbf{H}_{0\perp}$. Adding these two partial critical currents, then multiplying by 2, we obtained an estimate of I_c, in so far as the other three faces behave similarly. In practice, the symmetry of the faces is as difficult to achieve as the longitudinal homogeneity of the surface conditions. Despite this there was a fair agreement, within 10–20 %, between the surface critical current so estimated and I_c taken from the V-I curve. This given further evidence of the Joule heat VI_c arising essentially at the surface.

Let us return to Figs. 6 and 8. For clarity, the intercepts of the lines s_1 vs I and V vs I, at $s_1=0$ and $V=0$, have been denoted as I_s and I_c, respectively. As explained in Sec. II, I_c represents the longitudinal average of $I_c(y)$; in Fig. 6, $5\lesssim I_c(y)\lesssim 8$ A. The small observed difference between I_s and I_c is worth considering, even though it might be reasonably attributed to experimental errors. In particular, the separation of voltage probes ($\simeq 10$ mm) can hardly be determined to better than 1 mm, so that the cavity and the voltmeter may not explore exactly the same portion of the rod. Also, small differences in the phase of signals s_2 and s_3 may arise from corner effects (only available from a numerical 2D calculation), if the surface distributions of h and h_L sources do not coincide. As easily seen, this would entail a shift of I_s. Nevertheless, since I_s was systematically found to be smaller than I_c, we cannot rule out the possibility of a small bulk contribution to I_c. This occurrence should not weaken the bearings of our argument. Indeed, in increasing the cross section of the sample for experimental convenience, we risked enhancing bulk pinning, however weak it may be. Conversely, if 10–20 % of I_c is due to volume defects in rods having such a large cross section (16 mm^2), the bulk contribution to I_c in soft foils (0.1 mm thick) may be reduced to less than 1%.[2,3]

V. CONCLUSION

As has long been recognized, in the analog situation of rotation He II the obvious interest of continuum descriptions of the mixed state is to make the treatment of equilibrium and transport problems easier, whenever intricate deformations of the vortex array are involved, especially in the presence of defects. The originality of the MS theory, developed in this paper, essentially lies in stating and relying on the two fundamental equations (3) and (16), namely, the macroscopic London equation and the macroscopic equation for vortex equilibrium. Many earlier theories, in particular, the well-known elastic continuum theory,[1] restricted their attention to the sufficiently slow spatial variation that $\boldsymbol{\omega}$ and $\mathbf{B}$ were not discriminated, and the detailed distribution of currents, in connection with the local equilibrium of the VL, was ignored. On close examination it is seen that only a very restricted class of elastic deformations has been considered, i.e., those subject to the constraint $J_S\equiv 0$, $\boldsymbol{\omega}\equiv\mathbf{B}$. This considerably limits the field of possible solutions. In view of the extensive development of the elastic continuum theory in the literature, this criticism will be argued elsewhere.

As a simple application of the MS model, the magnetization of a perfect sample has been interpreted (Sec. II). Then the subcritical (Sec. II) and flux-flow properties (Sec. III) of soft samples have been investigated in detail. A surface pinning model (Sec. II) accounts for the magnitude of critical currents, and their field and temperature dependence. The surface mechanism responsible for the part VI_c of the Joule effect is elucidated, without having recourse to elastic instabilities. The existence of a surface Joule effect is demonstrated by the experiment of Sec. IV. As a consistent theory of flux-flow noise has long been challenging,[25] it should also be emphasized that a successful noise theory, supported by experiments,[12] proceeds from the MS model, as just mentioned in Sec. III. Subsequent papers are planned to be devoted to it.

Our grounds to pay particular attention to soft samples are explained in Sec. I. The theory of soft samples ap-

pears as an important step in understanding critical currents and dissipation, so far as it concerns a wide class of standard samples, as shown by experiment, and not fictitious samples completely free from volume imperfections.

One may wonder, however, at the frequent occurrence of the soft behavior, such as defined and described above. We can understand that volume defects are ineffective by a simple argument proceeding from Eq. (16). It will be noted that this argument has no connection with the notion of pinning threshold introduced in the elastic continuum theory,[1] which characterizes the strength of *one* pinning center. Suppose we are dealing with dilute point defects, in an otherwise perfect sample, including the surface. If the pinning sites are widely spaced on the scale of a, the continuum model still applies and Eq. (16) holds at equilibrium, in a simply connected domain excluding the pinning centers. Let $\mathcal{S}$ be a surface crossing the sample and lying entirely in this domain; the flux of $\mathbf{J}_S = -\text{curl}\varepsilon$ through $\mathcal{S}$, expressed as a contour integral (21) is zero. This means that such a sample cannot carry a supercurrent without dissipation, and $I_c = 0$. Now, by increasing the number of defects, the mean site spacing becomes comparable with a, so that the above argument fails, and then a net supercurrent can flow by some kind of percolation effect. Again we may speak of pinning threshold, but the latter is related to the defect concentration, irrespective of their strength.

[1] A. M. Campbell and J. E. Evetts, Adv. Phys. **21**, 199 (1972).
[2] W. C. H. Joiner and G. E. Kuhl, Phys. Rev. **163**, 362 (1967).
[3] B. Plaçais, P. Mathieu, and Y. Simon, Solid State Commun. **71**, 177 (1989).
[4] P. Thorel, Y. Simon, and A. Guetta, J. Low Temp. Phys. **11** 333 (1973).
[5] D. M. Kroeger and J. Shelten, J. Low Temp. Phys. **25**, 369 (1976).
[6] P. Mathieu and Y. Simon, Europhys. Lett. **5**, 67 (1988).
[7] I. L. Bekarevitch and I. M. Khalatnikov, Zh. Eksp. Teor. Fiz. **40**, 920 (1961) [Sov. Phys. JETP **13**, 643 (1961)]; I. M. Khalatnikov, *Introduction to the Theory of Superfluidity* (Benjamin, New York, 1965), Chap. 16.
[8] A. A. Abrikosov, M. P. Kemoklidze, and I. M. Khalatnikov, Zh. Eksp. Teor. Fiz. **48**, 765 (1965) [Sov. Phys. JETP **21**, 506 (1965)].
[9] B. D. Josephson, Phys. Rev. **152**, A211 (1966).
[10] C. R. Hu, Phys. Rev. B **13**, 4780 (1976).
[11] A. Schmid, Phys. Kondens. Mater. **5**, 302 (1966).
[12] B. Plaçais, Ph.D. thesis, Université Paris VI, 1990, p. 231.
[13] D. Saint-James, G. Sarma, and E. J. Thomas, *Type-II Superconductivity* (Pergamon, New York, 1969), Chap. 3, pp. 41–75.
[14] P. Mathieu, B. Plaçais, and Y. Simon, Phys. Rev. B **29**, 2489 (1984).
[15] P. Nozières and W. F. Vinen, Philos. Mag. **14**, 667 (1966).
[16] P. S. Swartz and H. R. Hart, Phys. Rev. **156**, 403 (1966); **156**, 412 (1966).
[17] R. E. Johnson and R. H. Dettre, J. Phys. Chem. **68**, 1744 (1964).
[18] R. G. Jones, E. H. Rhoderick, and A. C. Rose-Innes, Phys. Lett. **24**, 318 (1967).
[19] B. D. Josephson, Phys. Lett. **16**, 242 (1965).
[20] B. Plaçais and Y. Simon, Phys. Rev. B **39**, 2151 (1989).
[21] P. R. Solomon and F. A. Otter, Jr., Phys. Rev. **164**, 608 (1969).
[22] P. G. P. Weijenbergh and M. Van Beelen, Physica B **94**, 287 (1978); and references therein.
[23] Y. Simon and F. Vidal, Phys. Lett. **30A**, 109 (1969).
[24] F. Vidal, Phys. Rev. B **8**, 1982 (1973).
[25] J. R. Clem. Phys. Rep. **75**, 1 (1981).

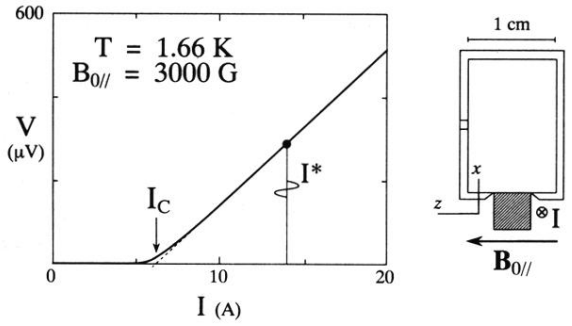

FIG. 6. A schematic of the fitting of a PbIn square rod on a rectangular second-sound resonator. Also shown is the measured dc voltage-current characteristic at 1.66 K, $B_{0\|}=3000$ G ($I_c=6.2$ A); the solid dot indicates the operating point for data reported in Fig. 7. A small superimposed ac current ($I^*\simeq 0.7$ A) modulates Joule and thermomagnetic heat sources. The sample acts as a second-sound transmitter and drives the cavity on its x fundamental mode, $\omega_0/2\pi\simeq 640$ Hz, at 1.66 K (quality factor 1650). A carbon bolometer (not shown) measures both amplitude and phase of the temperature oscillations. Its response (typically $\sim 10\,\mu$V) is amplified and directly plotted on the Argand plane, as shown in Fig. 7.